Contract No:

This document was prepared in conjunction with work accomplished under Contract No. DE-AC09-08SR22470 with the U.S. Department of Energy (DOE) Office of Environmental Management (EM).

Disclaimer:

This work was prepared under an agreement with and funded by the U.S. Government. Neither the U. S. Government or its employees, nor any of its contractors, subcontractors or their employees, makes any express or implied:

1) warranty or assumes any legal liability for the accuracy, completeness, or for the use or results of such use of any information, product, or process disclosed; or
2) representation that such use or results of such use would not infringe privately owned rights; or
3) endorsement or recommendation of any specifically identified commercial product, process, or service.

Any views and opinions of authors expressed in this work do not necessarily state or reflect those of the United States Government, or its contractors, or subcontractors.

Ni and Cr addition to alloy waste forms to reduce radionuclide environmental releases

L. Olson, SRNL

Reference alloy waste forms (RAW) were fabricated and underwent hybrid corrosion/immersion testing to parameterize the ANL analytical oxidative-dissolution model to enable the calculation of fractional release rates and to determine the effectiveness of Ni and Cr trim additions in reducing release rates of radionuclide surrogates. Figure 1 shows the prototypical multiphase microstructure of the alloys with each phase type contributing about equally to the exposed surface area. The waste forms tested at SRNL were variations of the RAW-6 formulation that uses HT9 as the main alloy component, and are meant to enable evaluation of the impact of Ni and Cr trim additions on the release rates of actinides and Tc-99. The test solutions were deaerated alkaline and acidic brines, ranging in pH 3 to pH 10, representing potential repositories with those conditions. The testing approach consisted of 4 major steps; 1) bare surface corrosion measurements at pH values of 3, 5, 8, and 10, 2) hybrid potentiostatic hold/exposure measurements at pH 3, 3) measurement of radionuclide concentrations and relations to anodic current from potentiostatic holds, and 4) identification of corroding phases using SEM/EDS of electrodes.

The RAW-6 alloys are similar to previous years RAW-3 alloys, but Ni and Cr concentrations varied between the 4 alloys made from ~0.4%-5.1%, and ~8.7%-11.2% (mass), respectively. The waste forms were labeled roughly per their Ni content: RAW-6(Ni1), RAW-6(Ni3), and RAW-6(Ni5). A total of 12 bare surface measurements were taken for each of the 3 alloys at each of the 4 pH conditions. Five hybrid experiments lasting about a week each were undertaken at pH 3 with the RAW-6(Ni3) alloy, with solution samples taken periodically throughout the testing to determine surrogate radionuclide release rates. Two series of measurements were run with the RAW-6(Ni3) alloy in which the potential was held for an hour while the current was observed to determine if the alloy was corroding or passivated so as to more accurately find the passivated corrosion potential. The FY16 tests, combined with earlier work, allow for a more definitive understanding of constituents beneficial to alloy stability in corrosive environments, and prediction of radionuclide release rates.

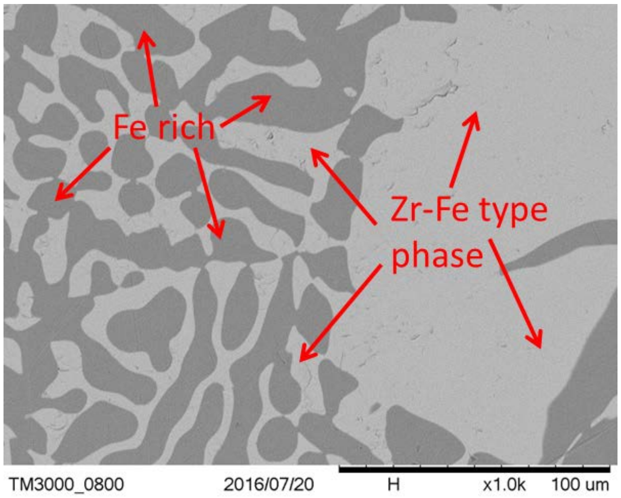

Figure 1 Prototypical multiphase microstructure of the alloy waste form surrogates. The lighter in color Zr-Fe phase is where actinides migrate too and the darker Fe rich phase where the Tc migrates. The degradation of the Fe rich phase and release of Tc is predicted to be the primary source of radionuclide release to the environment that may affect those at the boundary of a future repository. The focus of the multi-lab effort on alloy waste form degradation is to reduce corrosion of this phase.

Figure 2 shows the bare corrosion measurement and the end point corrosion currents (also shown in Table 1) that evolved during a week passivation at 5 different potentials from the RAW-6(3Ni) alloy in pH 3 solution. The anodic current is directly proportional to the net dissolution rate, and shows about an order of magnitude decrease within the first week for the region of the potentiodynamic scan dominated by the presence of Cr, with the lowest potential going into a fully passivated condition, and the highest point increasing into the transpassive region. EIS (not shown) was used to probe the surface stability of the electrode during the hybrid tests and detected the formation of a passivating layer for the three points with diminished corrosion currents (left of red line in Figure 2), and the loss of the protecting layer for the other two points. It is hypothesized based on the data that the passivation layer was reduced back to metal for the reducing condition but was not protective for the highest potential.

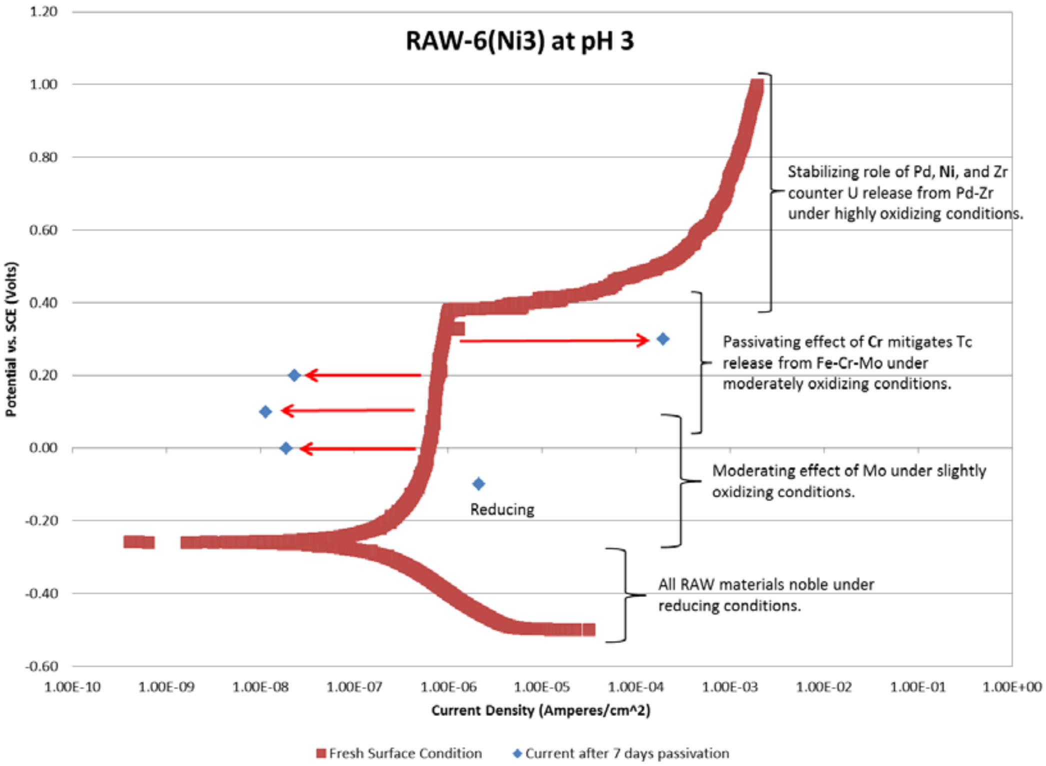

Figure 2 Potentiodynamic scan of RAW-6(3Ni). The potentiodynamic scan characterizes the bare surface of the freshly polished electrode. After a week of exposure to a simulated acidic groundwater, a characteristic passivating layer formed for that potential condition that resulted in reduced corrosion (release rates).

Table 1 Final current densities in RAW-6(Ni3) in pH 3 solution after 1 week hybrid potentiostatic hold/exposure experiments.

Hold potential (millivolts vs. SCE)	Final Current Density (Amperes/cm^2)
-100	2.13E-06
0	1.90E-08
100	1.15E-08
200	2.33E-08
300	1.95E-04

Figure 3 and Table 2 shows the specific alloying elements of interest that have leached into the test solution after about 1, 3, and 7 days of exposure to solution at the hold potential. Minimal release rates are observed for most of the hold potentials with the exception of the 300 mV hold potential that evolved into a transpassive regime.

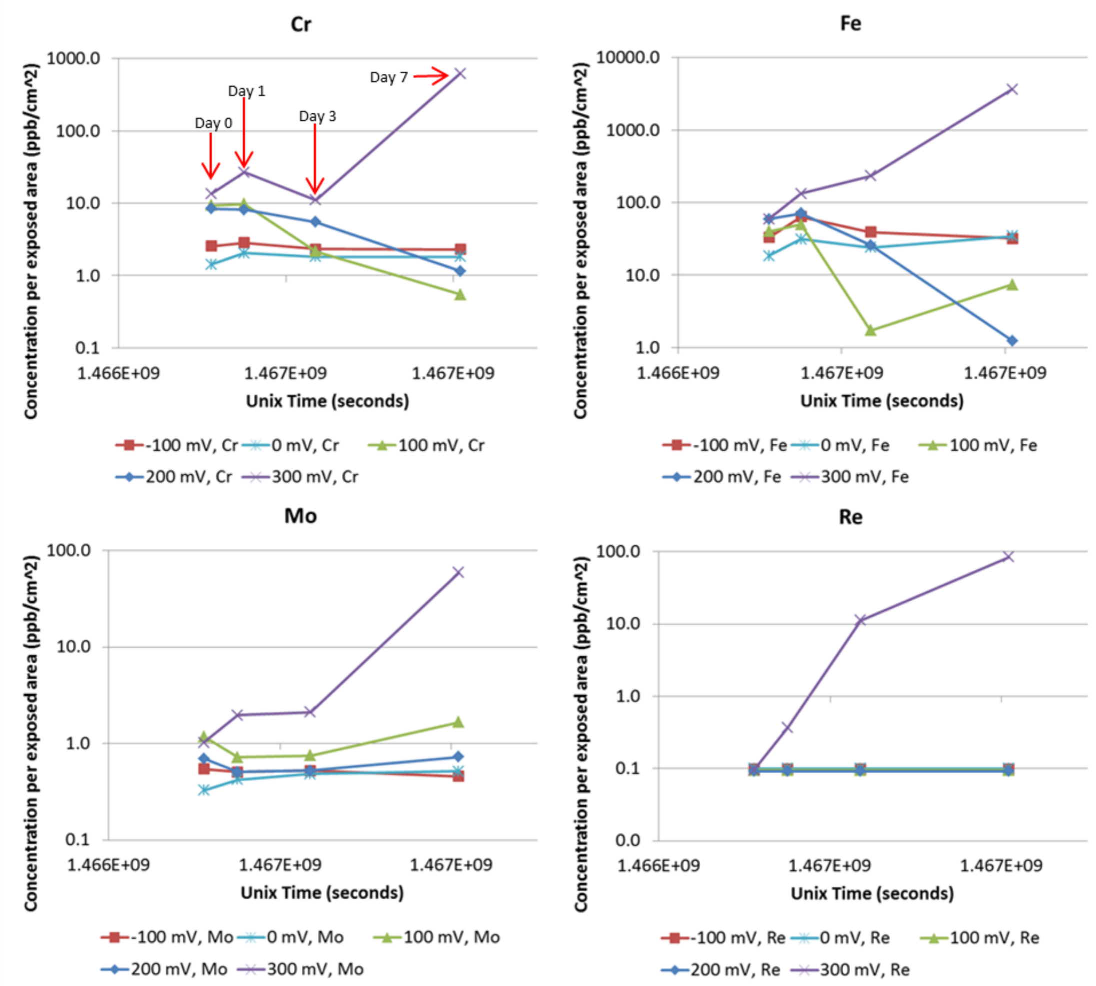

Figure 3 The concentration of Cr, Fe, Mo, and Re (Tc-99 surrogate), show negligible release from the alloy waste forms at all hold potentials except for 300 mV (vs. SCE).

Table 2 Concentration of Cr, Fe, Co, Mo, and Re are shown as a function of sampling time. Concentrations are per cm^2 of exposed alloy surface area.

		Concentration (ppb/cm^2)					
Hold Potential (mV vs. SCE)	Elapsed time since test start (hours:min:sec)	Cr	Fe	Co	Mo	Re	Cr
-100	0:00:00	2.5	32.9	0.2	0.5	0.1	2.5
	21:42:00	2.8	63.2	0.6	0.5	0.1	2.8
	68:58:00	2.3	39.1	0.3	0.5	0.1	2.3
	165:01:00	2.3	31.7	0.3	0.5	0.1	2.3
0	0:00:00	1.4	18.4	0.3	0.3	0.1	1.4
	21:10:00	2.0	31.1	0.5	0.4	0.1	2.0
	69:56:00	1.8	23.8	0.4	0.5	0.1	1.8
	162:29:00	1.8	34.2	0.4	0.5	0.1	1.8
100	0:00:00	9.3	39.8	0.2	1.2	0.1	9.3
	21:43:00	9.8	49.5	0.3	0.7	0.1	9.8
	69:00:00	2.2	1.7	0.1	0.8	0.1	2.2
	165:03:00	0.5	7.3	0.1	1.7	0.1	0.5
200	0:00:00	8.4	58.8	0.2	0.7	0.1	8.4
	21:12:00	8.1	70.4	0.1	0.5	0.1	8.1
	69:59:00	5.5	25.7	0.2	0.5	0.1	5.5
	162:31:00	1.1	1.2	0.1	0.7	0.1	1.1
300	0:00:00	13.6	59.1	0.2	1.0	0.1	13.6
	21:44:00	26.6	132.9	0.4	2.0	0.4	26.6
	69:01:00	11.0	232.5	0.3	2.1	11.2	11.0
	165:04:00	616.4	3658.0	0.2	59.3	84.5	616.4